Improvement of the mechanical and tribological behaviors by Ti-C interlayer for diamond-like carbon films on nitrile butadiene rubber

Wu, Yongmei; Liu, Jiaqi; Jiang, H.; Deng, Q.Y.; Wen, Feng; Pei, Yutao; Cao, Huatang

Published in:
Materials science and engineering b-Advanced functional solid-State materials

DOI:
10.1016/j.mseb.2023.116289

Materials Science and Engineering B 290 (2023) 116289

Contents lists available at ScienceDirect

Materials Science & Engineering B

journal homepage: www.elsevier.com/locate/mseb

Improvement of the mechanical and tribological behaviors by Ti-C interlayer for diamond-like carbon films on nitrile butadiene rubber

Y.M. Wu [a,d], J.Q. Liu [a], C.X. Han [a], H.T. Cao [b], H. Jiang [a], Q.Y. Deng [a], F. Wen [a,*], Y.T. Pei [c]

[a] Special Glass Key Lab of Hainan Province, School of Materials Science and Engineering, Hainan University, Haikou 570228, PR China
[b] State Key Laboratory of Materials Processing and Die & Mould Technology, School of Materials Science and Engineering, Huazhong University of Science and Technology, Wuhan 430074, PR China
[c] Department of Advanced Production Engineering, Engineering and Technology Institute Groningen, University of Groningen, Nijenborgh, 4, 9747 AG, the Netherlands
[d] Shanghai Branch of China Tower Corporation Limited, 201702, PR China

ARTICLE INFO

Keywords:
Rubber
Ti-C interlayer
DLC/Ti-C bilayer
Nanoindentation
Tribology

ABSTRACT

To improve the mechanical and tribological properties of diamond-like carbon (DLC) film on nitrile butadiene rubber, the DLC/Ti-C bilayer films are fabricated by a dual-target magnetron sputtering method. The morphological characterization results indicate that the roughness of DLC/Ti-C first decreases and then increases slightly with the increase of Ti content and surface roughness of all modified samples is lower than that of nitrile butadiene rubber (NBR). Raman spectra show that the change of Ti content in the Ti-C interlayer has no effect on the ratio of sp^2 to sp^3 bonds of surface DLC film. The nanoindentation results show that the Ti content significantly affects the hardness, Young's modulus, h_{rex}/h_{max} and elastic recovery (%). Notably, the DLC/Ti-C films with a Ti content of 12.32 ~ 14.77 at. % show the lowest coefficient of friction (CoF, 0.1 ~ 0.2) and superior wear resistance due to the increased transformation of sp^2 into sp^3 in the films. This study unravels that the DLC films' superior mechanical and tribologic performance could be realized by regulating the Ti content in the Ti-C interlayer.

1. Introduction

Diamond-like carbon (DLC) films are characteristic of superior mechanical properties (such as high hardness, chemical inertness etc.) and excellent tribological properties (high wear resistance and ultralow friction coefficient) [1]. They have attracted increasing attention as a protective film to promote the tribological performance of rubber seals [2]. Nevertheless, the DLC films usually produce high residual stress at the interface of DLC/rubber in the growth process [3] because of the different thermal expansion coefficients between DLC and rubber and the low adhesion property of DLC on rubber. The nitrile butadiene rubber (NBR) seals utilized in engineering applications usually suffer from high friction and severe abrasion wear, causing substantial material loss and eventual failure of the lubrication system. The functionality of optimized hard films usually depends on developing a multilayer with a gradient architecture where the adhesion, load support, and low friction regions are the crucial factors [4,5]. Incorporating metal elements into carbon matrix such as Ti could result in an excellent adhesion to rubber substrate. Notably, the easy reaction tendency of Ti with carbon to form TiC nanocomposites in an amorphous carbon (a-C) matrix adds flexibility for the film [6,7].

Moreover, the formation of Ti compounds acts as a buffer layer, which could facilitate the conversion of physicochemical properties. Such a gradient composition and structure design can effectively minimize the difference in physical behaviors [8]. Therefore, the hard yet lubricating DLC films coated on rubber substrates may have good adhesion strength, which can flexibly adapt to the immense strain of NBR seals under loads and improve the mechanical properties for the potential surface engineering applications [9]. Many studies focused on Ti-doping of DLC films to investigate whether titanium atoms are saturated in the a-C matrix or exist in the form of TiC nanocrystallites [10–12]. However, there are only a few reports on using a Ti-C interlayer to improve the mechanical properties of DLC thin films deposited on elastomer materials.

There have been many approaches to preparing DLC films over the past decades. Magnetron sputtering (MS) has many advantages, such as high deposition efficiency, low deposition temperature, and large-area deposition. It has been widely applied in the deposition of various

* Corresponding author.
E-mail address: fwen323@163.com (F. Wen).

https://doi.org/10.1016/j.mseb.2023.116289
Received 8 October 2022; Received in revised form 9 January 2023; Accepted 15 January 2023
Available online 13 February 2023

advanced films, such as superhard films, ultralow friction and wear-resistant films, corrosion-resistant films, and decorative films in industries [8,13–15]. In our previous work [16], we focused on studying the effect of substrate bias on composition and structure of Ti-C interlayers and tribological properties of DLC films prepared on rubber. The present work prepared the DLC/Ti-C bilayer films with different Ti contents on nitrile butadiene rubbers by power modulation. The effects of Ti content in the Ti-C interlayer on the microstructure, tribology, and microhardness of DLC-coated NBR rubbers was studied.

2. Experimental details

2.1. Preparation of DLC/Ti-C films

A set of DLC/Ti-C films were deposited on a NBR sheet (Shore A 65, 20 mm × 20 mm × 6 mm) by dual-target magnetron sputtering with an argon flow. The NBR rubbers were cleaned by soap and hot deionized water for 10 min in an ultrasonic cleaner to remove the contaminations on the rubber surface (such as oil and grease). Then the substrates were dried in a vacuum oven at 90 degrees under room pressure for 15 min. We used a pressed sheet fixation method in the vacuum bin to keep it stable. While NBR samples were laid flat on the holder, silver paste was used between the back center and holder. Simultaneously, the back of the four corners of the NBR was also connected with the holder with silver paste. The schematic is shown in Fig. 1. In this way, positively charged ions can be loaded onto the sample surface as much as possible. The base pressure of the deposition chamber was 3.0×10^{-3} Pa. Next, the specimens were etched in Ar plasma bombardment for 5 min at a negative bias voltage of 600 V (40 kHz frequency, 75% duty ratio) to remove the surface oxide contamination and fostered the adhesion with the substrate. A Ti-C interlayer was firstly deposited with dual-target sources, namely, one circular graphite target (Φ76.2 mm × 4 mm, 99.99 % purity) powered by direct current magnetron under 100 W and one circular titanium target (Φ76.2 mm × 4 mm, 99.99 % purity) powered by radio frequency magnetron under different power conditions and bias voltage to control Ti content. Subsequently, DLC films were deposited on the Ti-C interlayer by DC magnetron sputtering with the bias of −100 V. The flow rate of argon gas was fixed at 30 sccm and the working pressure was kept at 2.0 Pa. The detail deposition parameters were seen in Table 1.

2.2. Characterization of multilayer films

The structure of DLC/Ti-C films was analyzed by Raman spectroscopy (Nano Finder 30A, Tokyo Instruments, INC) with a 532 nm laser. The uniformity of the films was analyzed by Raman mapping on an area of 100 μm × 100 μm for further observation. A 50 × objective lens was used. The laser power was controlled at 1 mW to enhance the signal strength of the film. The Raman mapping test was done in an automated platform in terms of point-by-point. The key parameters were recorded as follows: the step space was set as 10 μm and the integration time was set as 8 s. The Raman spectra from 1000 cm^{-1} to 2200 cm^{-1} was recorded.

The surface roughness (10 μm × 10 μm) of the deposited NBR samples was investigated by atomic force microscope (AFM, Nanosurf AG, Tap 90AL-G) in the tapping mode. According to previous work, the thickness of the prepared DLC film is approximately 200 nm and the thickness of the Ti-C layer is equal to or slightly thicker than that of the DLC film. The total film thickness is therefore approximately 400 nm [16]. The hardness and Young's modulus of the films were investigated by a nanoindenter (CETR-UMT, Bruker) equipped with a Berkovich diamond tip. The load continuously increased up to a maximum of 1 mN within 15 s, and then held for 10 s followed by unloading progress within 15 s. The thermal drift procedure was kept with a fixed load for 45 s during the unloading to 0.1 mN. Five random tests were tested in each sample. Each two indentations were spaced by 20 μm to eliminate possible influence of residual stress from the adjacent indentations. The triboperformance of the films was evaluated by a ball-on-disk tribometer (CETR-UMT, Bruker) under ambient conditions (45% R_H) at room temperature. A commercial zirconium oxide ball of Φ1.6 mm was selected as a counterpart under a normal load of 0.3 N, and the test parameters were as follows: the circular path was 9 mm in diameter, the speed was 100 rpm, and the sliding time was 120 min. Afterward, the wear tracks were examined by SEM (TESCAN MIRA3).

3. Results and discussion

Surface topography of the as-deposited films (5.45 at.%, 12.32 at.%, 13.49 at.%, 14.77 at.% , 31.61 at.%) were observed by AFM, as seen in Fig. 2. The results show that all modified samples have lower surface roughness compared to NBR's surface. And the surface roughness of DLC/Ti-C films on the rubber varies as the Ti content increases. It is clear that the surface roughness first decreases and then increases slightly with the increase of Ti content. This is ascribed to the plasma ionization

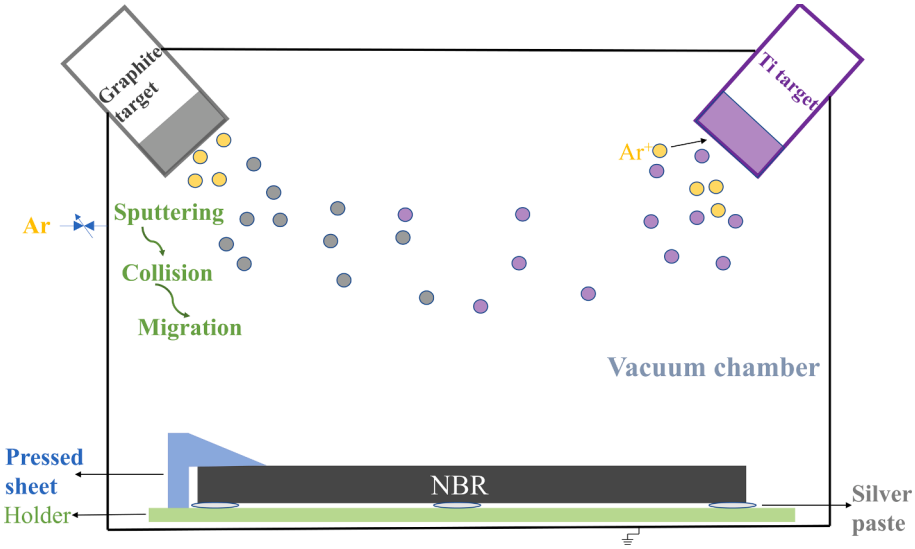

Fig. 1. Schematic plot of NBR fixture while deposition.

Table 1
Deposition parameters and chemical compositions of DLC/Ti-C films on NBR.

Film No.	Ti-C interlayer					DLC film		
	SubstrateBias(V)	Ti target power (W)	Deposition time (min)	Composition (at. %)		Substrate bias (V)	C target DC power (W)	Deposition time (min)
				C	Ti			
5Ti	0	80	10	94.55	5.45	100	100	30
12Ti	150	80		87.68	12.32			
13.5Ti	150	120		86.51	13.49			
15Ti	150	140		85.23	14.77			
32Ti	250	140		68.39	31.61			

density and the energy atoms in the scattering process. Different numbers of sputtered atoms collide, resulting in different surfaces on the Ti-C layer, and the surface roughness of DLC deposited on various Ti-C layers is varied. As can be seen, the film with a content of 12.32 at. % Ti shows a typical worm-like morphology, while the film with a content of 13.49 at. % and 14.77 at. % Ti shows denser surfaces and atom clusters characterization. This is because the target power with a higher power produces more atom energy and the high energy helps the films form cluster-like structures. This facilitates the atom's re-sputtering and thus presents different morphologies.

Fig. 3 shows the typical Raman spectra of the DLC/Ti-C films deposited on the NBR in the range of 800–2000 cm^{-1}, showing the prominent G and smaller underlying D peaks (centered at approximately 1580 cm^{-1} and 1350 cm^{-1}, respectively), which corresponds to the stretching vibration of any pair of sp^2 bonds whether in chains or in aromatic rings and the breaking mode of sp^2 bonds only in rings, respectively [17]. Generally, Raman results show that the symmetry center of the main peak basically remained unchanged when the negative bias increased, indicating that the degree of graphitization of the DLC film was constant and the internal components of the DLC have not changed significantly. Briefly, supposing the symmetry of the Raman spectrum is weakening as the G peak widens, the film structure tends to be graphitization [3]. In addition, we investigated that the Ti content in the Ti-C interlayer has no effect on the symmetry center of the G-peaks, ensuring that the Ti content is the main cause of the film properties in subsequent tests.

The uniformity of DLC/Ti-C samples with different Ti contents (12.32 at. %, 13.49 at. % and 14.77 at. %) were further analyzed by Raman mapping, as seen in Fig. 4. For films in 10 μm × 10 μm regions, the color distribution of them is relatively uniform, indicating a uniform chemical structure at micro-scale [17]. It should be pointed out that the homogeneity of films is mainly due to the high-energy particle impingement onto the NBR substrate, which increases the degree of sample ionization at lower energy, thereby densifying the films substantially. The Raman mappings confirmed that the DLC/Ti-C films with the Ti content at 12.32 at. %, 13.49 at. % and 14.77 at. % maintained uniformity. We made the curve of I_D/I_G (intensity ratio) based on the mapping picture of D and G peaks, seen in above Fig. 4d. The average I_D/I_G are 0.94, 0.94, and 0.95, respectively, which shows the good homogeneity of films' composition. The I_D/I_G values of the films do not differ much, indicating that the influence of sputtering power on the film surface uniformity is insensitive.

Fig. 5 shows the load versus displacement curves at maximum indentation load for DLC/Ti-C films under different Ti contents. The process is divided into three stages: loading, holding, and unloading. It is noteworthy that the unloading process shows creep due to the viscous flow and elasticity behavior of rubber substrate, which may result in a high value of Young's modulus [18]. Consequently, considering the viscoelastic properties of the polymeric materials, we held the indenter at the maximum indentation load of 1 mN for 10 s. A typical load versus displacement curve is shown in Fig. 5, which has been rectified for thermal drift, and the curve exhibits parabolic loading and power-low unloading [19]. With increasing load and depth, the indenter goes from the DLC interface to the Ti-C layer and then from the Ti-C layer to the substrate, has different hardness and modulus at different interfaces. It can be seen from the curves of load vs. depth, a discontinuity can be observed at the end of loading and the beginning of unloading, that is, at large depth. This may be attributed to the phase transformation in the films. During unloading, it can be observed that the varied hysteresis curve and the maximum indentation depth (h_{max}) are also significantly different as the Ti content increases. The Oliver-Pharr method was employed to calculate the hardness and Young's modulus of the films [20]. After unloading, it's worth noting that the indentation rebound depth is over 800 nm, exceeding the thickness of the film. Thus, the value of hardness is considered as the combined hardness of the DLC/Ti-C film and the rubber substrate. The NBR seals in the practical applications usually suffered from frictional losses, and the films are used to improve the wear resistance of the substrate. Thus, the composite hardness and modulus of thin film are more practical.

Fig. 5a is the unloading schematic, Fig. 5b is the load-depth curves of NBR with DLC/Ti-C bilayer films under different Ti contents. It can be seen from Fig. 5b, the h_{max} values of the samples at 5.45, 12.32, 13.49 and 31.61 at.% Ti content exhibit larger depths and they are significantly higher than that of 14.77 at%; while the residual depth (h_{res}) of all samples are roughly similar. Moreover, it can be found that the h_{res} trend of the samples is consistent with the h_{max} under different Ti contents. According to a previous study, the magnetron sputtering may enhance DLC characteristics of the samples that manifested in the hysteresis, penetration depth, residual penetration depth and the observed recovery [21], which could help the DLC film to better combine with the soft substrate of rubber.

Table 2 shows the hardness (H) and Young's modulus (E) values of NBR for Ti-C / DLC bilayer films deposited under different Ti contents. The hardness and Young's modulus of the films considerably differ under different Ti contents. The hardness variation trend tracks with Young's modulus. In the case of Ti content at 5.45 at. %, the sample shows the highest hardness value and Young's modulus, 19.2 MPa and 72 MPa, respectively. While the sample exhibits the lowest hardness value and Young's modulus as the Ti content increased to 31.61 at. %, namely, 6.8 MPa and 19.6 MPa, respectively. The H and E of hydrogen-free DLC films have been influenced by the carbon bonding configuration [22]. The decrease in H and E of the films is associated with the formation of aromatic bonds induced by less energetic deposition processes due to increased Ti contents. This is in good accordance with the Raman results in Fig. 3. When the Ti content in the Ti-C interlayer is 12.32 ~ 14.77 at. %, the hardness of the sample fluctuates from 9.80 MPa to 7.83 MPa, and simultaneously the Young's modulus range is from 50.60 MPa to 42.83 MPa. The results show that the Ti content in the transition layer affects the hardness and the Young's modulus. This is consistent with the report that a thin interlayer could increase the hardness and toughness of a multilayered nanostructure [23].

The load-depth curves are not only used to determine the hardness (H), Young's modulus (E), but also to reflect the ratio of residual displacement (h_{rex}/h_{max}), elastic recovery (ER), the elasticity index (H/E) and the plasticity index (H^3/E^2) of the samples. The H/E is related to the absorb energy elastically, a high H/E is able to resist the substrate

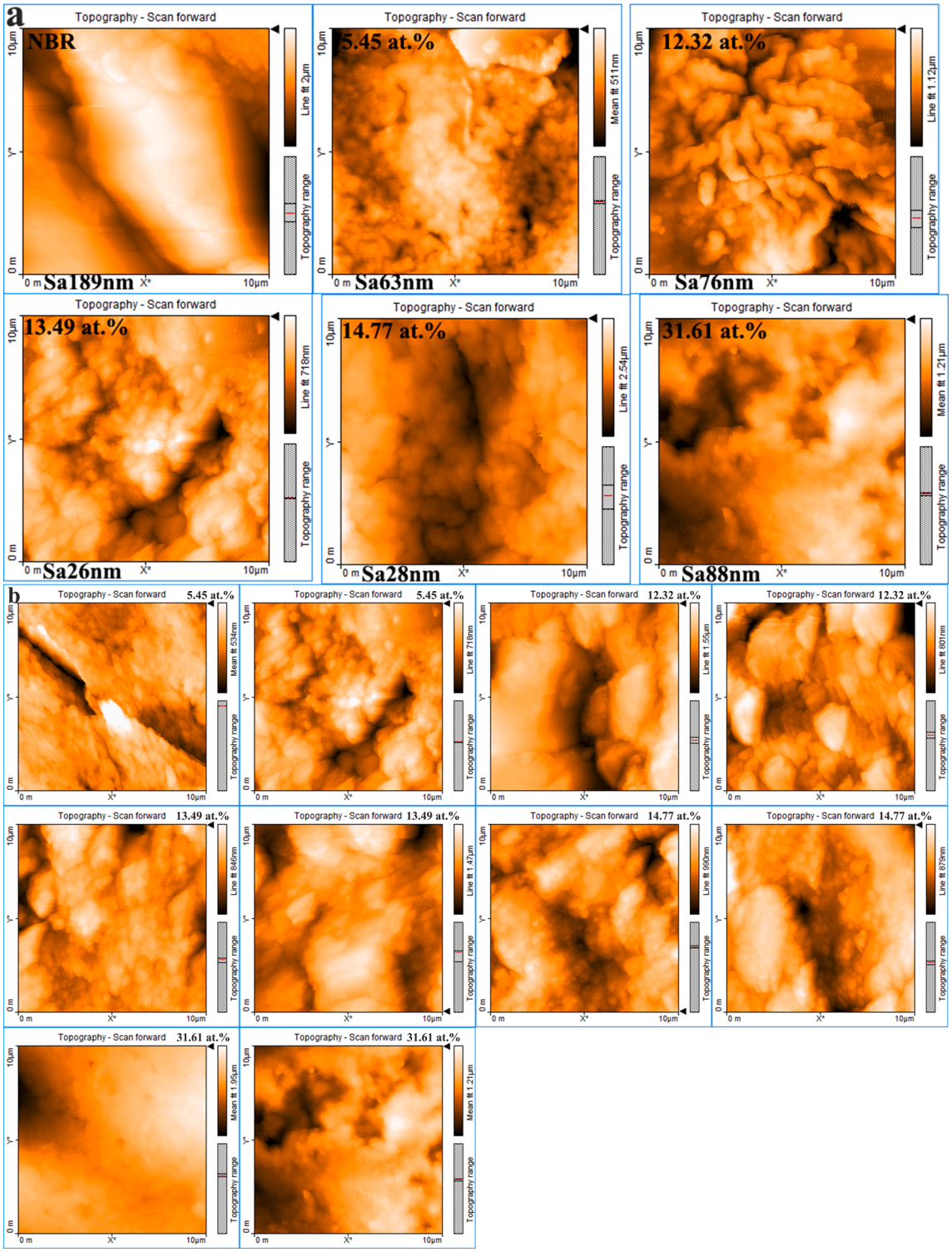

Fig. 2. (a) AFM images (10 × 10 μm^2) of the DLC/Ti-C films with the Ti content at 5.45 at.%, 12.32 at.%, 13.49 at.% and 14.77at.%. (b) AFM images in different areas of DLC/Ti-C films.

deformation under an applied load without fracture [24]. The H/E ratio variation of DLC/Ti-C films on NBR ranges from 0.18 ~ 0.34. The higher value of H/E ratio in the samples, the lesser the elastic deformation will occur. The H/E ratio of the sample (5.45 at. % Ti content) is 0.27, which is related to the increased fraction of the mechanical work dissipated during plastic deformation [25,26], indicating the higher wear resistance for elastic materials such as rubber substrate. Instead, the film with a high Ti content of 31.61 at. %, the H/E ratio increases to 0.34. This is closely associated with the higher content of sp^3 bonding in the sample with 31.61 at. % Ti. For the rubber substrate, it may easily lead to the deformation of film and even cause the film to peel off.

Compared with H/E, the H^3/E^2 is more sensitive to the modulation period. The H^3/E^2 ratio can be used to characterize the material's resistance to plastic deformation [27,28]. It is reported that the ratio of H/E and H^3/E^2 can be used to evaluate the resistance to elastic deformation and plastic deformation of the membrane, respectively [29].

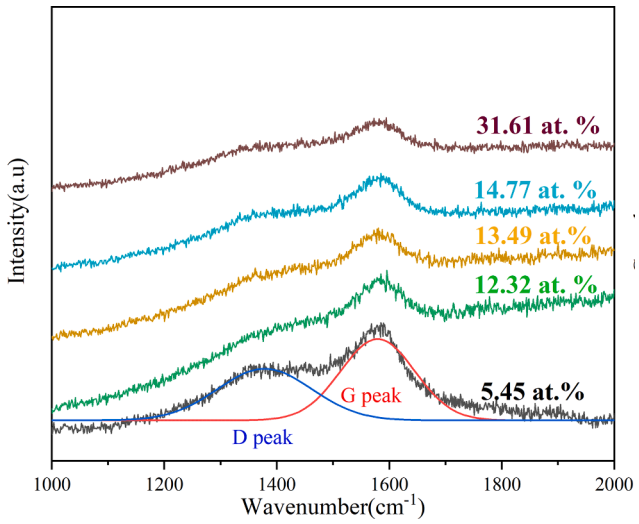

Fig. 3. Raman spectra of the DLC films with Ti-C interlayer deposited on NBR at different Ti contents.

From Table. 2, it can be seen that the H^3/E^2 ratio is downshifting from 1.37 to 0.26, as the Ti content increases from 5.45 at. % to 12.32 at. %. With further increasing Ti content, the H^3/E^2 ratio increased to 0.82. These results are in good accordance with the H/E value. The increase of Ti content decreases both the H/E and H^3/E^2 ratio, indicating an aggravated deformation and wear resistance of the thin films. It is recognized that these two parameters of the films are as significant as the hardness in determining the wear resistance (in abrasion, impact, and erosive wear in particular). Therefore, the DLC/Ti-C films with the optimized hardness, the H/E and H^3/E^2 are supposed to have enhanced wear resistance. ER and h_{res}/h_{max} are very important mechanical parameters, which are closely associated with the elastic and plastic behaviors, and therefore to the films [30]. The ER of the deposited samples can be calculated by the Eq. (3–1):

$$ER = \frac{(h_{max} - h_{res})}{h_{max}} \times 100\% \quad (3\text{-}1)$$

The h_{rex}/h_{max} and ER values for different Ti content samples are also shown in Table 2, i.e., the ER are in the range of 64 % to 79 %, and the h_{rex}/h_{max} ratio variation is 0.21 ~ 0.29, indicating the plastic behavior of films. The h_{rex}/h_{max} closely tracks with ER results, similar to the H/E and H^3/E^2 values. Generally, the mechanical properties of the samples are strongly related to the surface roughness, the carbon structure and the Ti content in the interfacial transition layer. The difference in the mechanical response of the rubber substrates significantly affects the tribological behaviors of the coated rubbers [8].

Fig. 6 shows the coefficient of friction (CoF) curve of NBR and DLC/Ti-C-coated films coated on NBR under different contents of Ti. As can be seen, the raw NBR exhibits the highest CoF (around ~ 1.1), while the

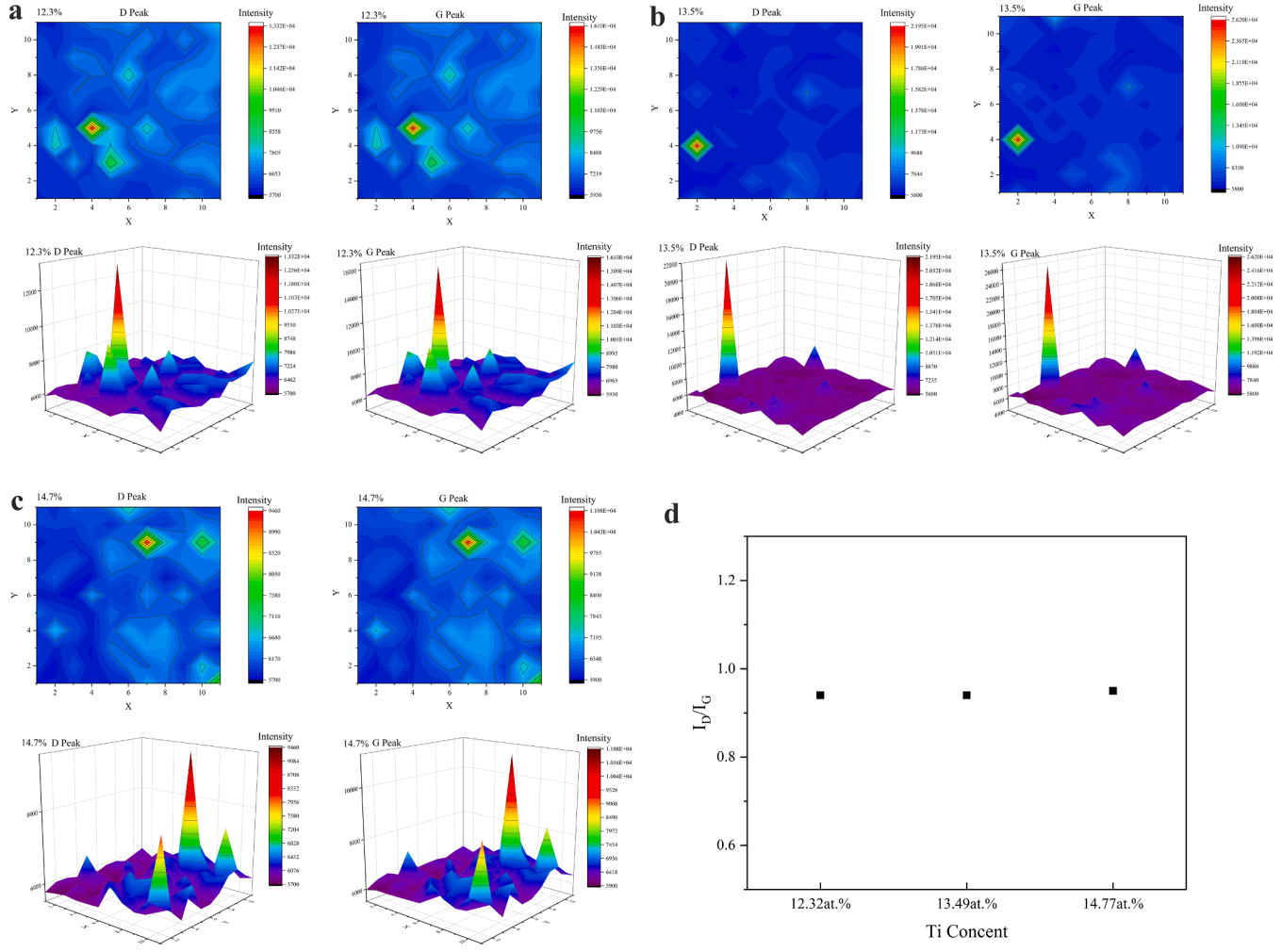

Fig. 4. The Raman mapping images (the horizontal and vertical coordinates represent the size of the area, which is 10 μm × 10 μm) of the DLC/Ti-C films deposited on the NBR with the Ti content at (a) 12.32 at. %, (b) 13.49 at. %, (c) 14.77 at. % and (d) I_D/I_G of Raman spectra based on the mapping picture of D and G peaks.

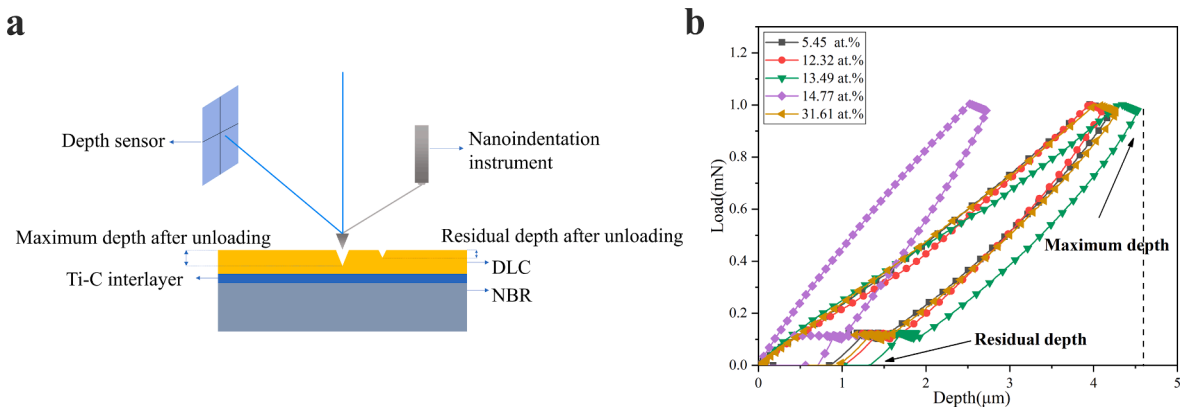

Fig. 5. (a) unloading schematic, (b) the load-depth curves of NBR with DLC/Ti-C bilayer films under different Ti contents.

Table 2
The value of H, E, H/E, H^3/E^2, h_{rex}/h_{max} and ER of DLC/Ti-C coated on NBR.

Film. No	H / MPa	E /MPa	H/E	H^3/E^2	h_{rex}/h_{max}	ER (%)
5Ti	19.2	72.00	0.27	1.37	0.26	74
12Ti	9.00	45.50	0.20	0.35	0.20	64
13.5Ti	9.80	50.60	0.20	0.36	0.21	78
15Ti	7.83	42.83	0.18	0.26	0.20	79
32Ti	6.80	19.60	0.34	0.82	0.29	71

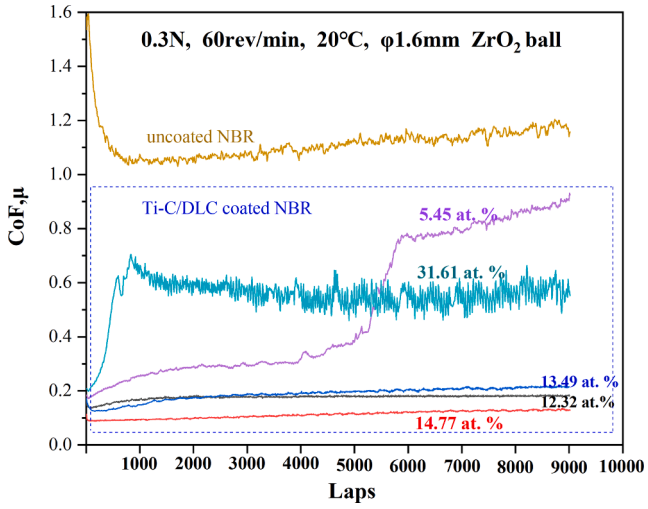

Fig. 6. Tribological behavior of NBR, DLC and DLC/Ti-C-coated films on NBR.

CoF of DLC/Ti-C-coated NBR decreases rapidly with the varied Ti content. The decreased CoF indicates that DLC/Ti-C can significantly improve the tribological performance of NBR rubber. The film with a low Ti content of 5.45 at. % shows a low CoF of ~ 0.27 at the beginning of 5000 laps, and the CoF rapidly increases to ~ 0.89 at 9000 laps, indicating a poor adhesion and rapid failure of the film. When the Ti content is low, the mechanism would be dominated by the DLC films because the contribution of the a-C matrix is over those of the TiC nanocrystallites [27]. Compared to the film with a low Ti content of 5.45 at. %, it is clear that the CoF increases to the value of ~ 0.67 after 1000 laps and finally keeps at ~ 0.65 as 31.61 at. % Ti content. These results may be attributed to the differences in Ti content and the adhesive interaction and hysteresis. The friction-induced heating facilitates the formation of the graphitized transfer layer, which decreases the friction of films [26]. When the Ti content in the transition layer ranges from 12.32 at. % to 14.77 at. %, the CoF is maintained at a relatively stable value of around 0.1 ~ 0.2 after 9000 laps. The low CoF is mainly attributed to the Ti-dopped carbon interlayer that destabilizes the carbon structure as the Ti content increases. Moreover, the film at this time has good mechanical properties, suitable toughness and strong resistance to plastic deformation. During the tribotest, the roughness of the films has a positive effect on its frictional characteristics because of the friction reduction in the contact area [24]. These results reveal that the samples with a relatively Ti content (31.61 at. %) or a relatively low Ti content (5.45 at. %) lead to high CoFs and poor wear resistance.

According to the curve of CoF, the films with the Ti content ranging from 12.32 at. % to 14.77 at. % exhibit low CoF and good wear resistance. SEM images in Fig. 7 show that the tribological morphologies of DLC/Ti-C films deposited on NBR with different Ti contents (5.45 at. %, 12.32 at. %, 13.49 at. %, 14.77 at. % and 31.61 at. %). The wear tracks of these samples are invisible with no apparent damage. The few microcracks formed in films are ascribed to the large elastic deformation of rubber substrate, indicating excellent wear resistance and high adhesion strength. The reason is that the physical linking by the Ti-C interlayer and interlocking promote the adhesion of the film. Besides, the different friction responses can be explained by the different chemical reactions in the contact process caused by the friction mechanism [28]. Rotational friction causes viscoelastic deformation of the soft film and the hard substrate, in addition, there is a large difference in the coefficient of thermal expansion between rubber and DLC. All these lead to the generation of microcracks on the film surface.

Fig. 7 shows the high-magnification SEM images of wear scar of NBR substrate and DLC/Ti-C-coated NBR samples under different Ti contents as indicated (5.45 at. %, 12.32 at. %, 13.49 at. %, 14.77 at. % and 31.61 at. %) and the surface morphology of raw NBR substrate was also shown in Fig. 7j. From Fig. 7, the texture of NBR rubber surface can be observed and the tribological properties of NBR before and after DLC/Ti-C modification can be studied. It can be seen that no evident damage was observed when the Ti content is 12.32 at. %, 13.49 at. % and 14.77 at. %. Although dense crack networks do exist in as-deposited raw films, the wear tracks of DLC/Ti-C films on the NBR rubbers do not exhibit any trace of delamination and fracture after tribotest. Consequently, a low, stable CoF (as shown in Fig. 6) of 0.1 ~ 0.2 is obtained in the DLC/Ti-C film with the Ti content of 12.32 at.%, 13.49 at. % and 14.77 at.%, and debris is undetectable on the DLC/Ti-C films. Note that the wear crack concave is towards the sliding direction of the counterpart ball. According to previous studies, the wear mechanism is mainly governed by the self-lubricating effect of amorphous carbon via the transformation of sp^3 bonding to sp^2 bonding itself due to the accumulation of friction heating [30,31]. Moreover, the DLC-coated films with Ti content of 5.45 at. % and 31.61 at. % peeled off completely from the raw NBR rubber substrate due to the poor adhesion behavior of the film. These results match well with the CoF in Fig. 6.

The substrate surface roughness is a significant parameter that affects the surface wettability and the tribological behavior of films. To

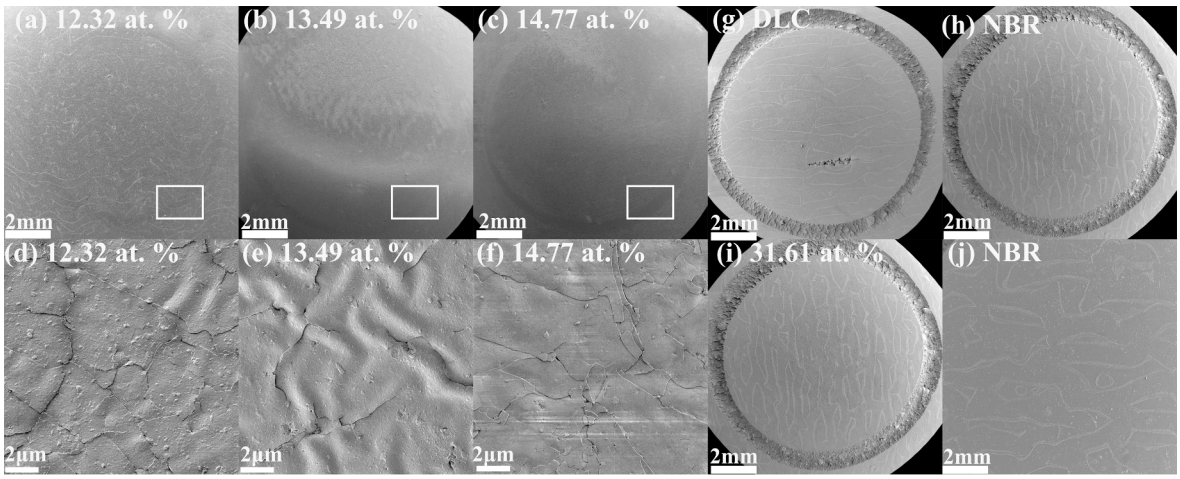

Fig. 7. SEM images of the wear scar of the samples with different Ti contents (i.e., DLC/Ti-C-coated on NBR) and bare NBR: (a) and (d) 12.32 at. %, (b) and (e) 13.49 at. %, (c) and (f) 14.77 at. %, (g) 5.45 at. %, (i) 31.61 at. %, and (h, j) the raw NBR.

clarify the influence of Ti contents on mechanical properties and the tribological behaviors, the CoF and arithmetical mean height (Sa) as a function of Ti content were plotted, shown in Fig. 8(a). It can be observed that the DLC/Ti-C films with a lower roughness induce a lower CoF, and the Sa is in good accordance with the CoF variations. The Sa is 63 nm and 86 nm when the Ti content in the thin film is 5.45 at. % and 31.61 at. % (shown in Fig. 2), respectively. A significant increase in the roughness of film leads to a smaller contact area of counterpart, thereby generating a higher CoF and weak wear resistance. This suggests that the effect of roughness on wear can be expected to be determined by abrasion in most cases [32]. The lower surface roughness reduces the CoF by inhibiting the generation of wear particles, removing the wear particles from the sliding interface and avoiding their agglomeration [31]. It should also be pointed out that higher contact stress on a rougher surface during sliding may aggravate the failure of the film [33]. Fig. 8(b) shows the relation between the mechanical property parameters (H^3/E^2 and h_{rex}/h_{max}) and the CoF of DLC/Ti-C films with different Ti. The H^3/E^2 and h_{rex}/h_{max} are in good agreement with CoF as the Ti content increases. The plasticity index H^3/E^2 is associated with the wear resistance of the material to plastic deformation [27]. In the case of Ti content at 5.45 at. %, the sample shows the highest CoF, h_{res}/h_{max} and H^3/E^2, suggesting the highest plasticity. This result indicates the lower plastic deformation of the superhard film on the elastomer materials. Consequently, the DLC/Ti-C film with low Ti content is easy to peel-off from the rubber substrate, leading to high friction and severe wear of films.

In contrast, the proper Ti contents (12.32 at. %, 13.49 at. % and 14.47 at. %) may well adapt the high resistance to the deformation during tribotest. The poor adhesion and low hardness exhibited on the DLC/Ti-C films may be attributed to the lower sliding life and higher wear rate. These films show superior triboperformance because the appropriate Ti content in the Ti-C interlayer optimizes the films' adhesion, flexibility, hardness, and wear resistance, resulting in improved mechanical properties. In practical applications, poor adhesion will lead to early film failure due to the substantial material loss caused by wear. Overall, the Ti content in the Ti-C interlayer is significant in adjusting the triboperformance of coated rubbers, and the design of Ti-C interlayer on an elastic substrate may play a critical role in enhancing the film flexibility and adhesion with the substrate.

4. Conclusions

The DLC/Ti-C films on NBR with different Ti contents were fabricated by dual-target magnetron sputtering. Compared to the raw rubber, the DLC/Ti-C films exhibit superior triboperformance when the Ti content is 12.32. %, 13.39 at. % and 14.47 at. %, which is attributed to the low CoF, high hardness and good uniformity of the DLC/Ti-C films via the introduction of Ti into the Ti-C interfacial transition layer. In particular, the interlayer design appreciably improves mechanical properties and increases wear resistance in tribological applications.

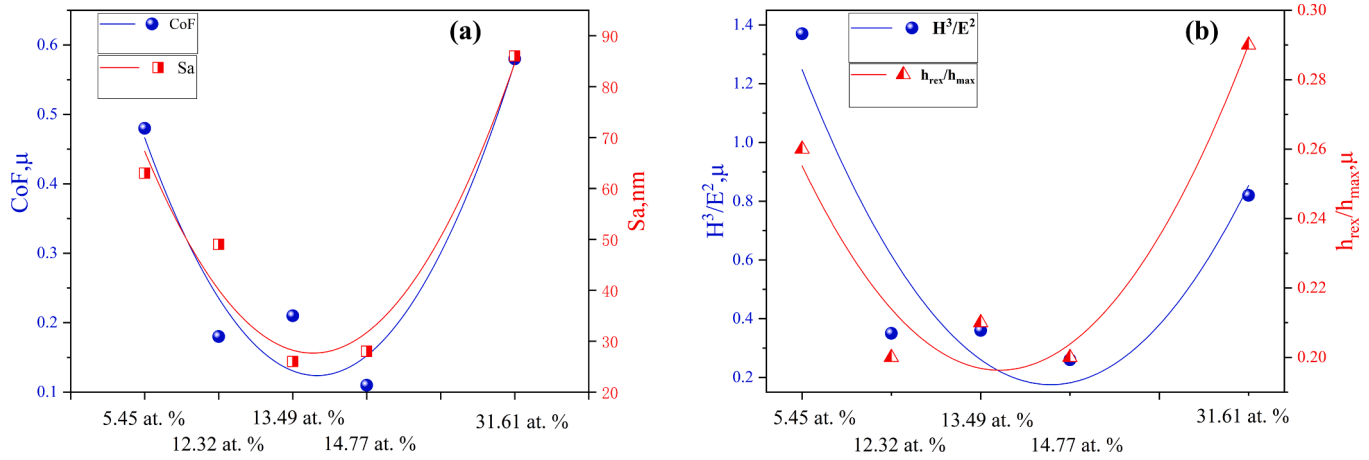

Fig. 8. (a) Relation curve between the surface roughness value Sa and CoF, and (b) the relation curve on the mechanical properties parameters of H^3/E^2 and h_{rex}/h_{max} under different Ti contents (5.45 at. %, 12.32 at. %, 13.49 at. %, 14.77 at. % and 31.61 at. %).

Declaration of Competing Interest

The authors declare that they have no known competing financial interests or personal relationships that could have appeared to influence the work reported in this paper.

Data availability

Data will be made available on request.

Acknowledgement

This project is supported by the Hainan Province Science and Technology Special Fund (ZDYF2019206) and the Natural Science Foundation of Hainan Province (420RC525).

References

[1] J. Robertson, Diamond-like amorphous carbon, Mater. Sci. Eng. R Reports 37 (4) (2002) 129–281.
[2] Y. Aoki, N. Ohtake, Tribological properties of segment-structured diamond-like carbon films, Tribol. Int. 37 (11) (2004) 941–947.
[3] Y. Xu, J.H. Jiang, G.G. Zhang, H.C. Li, T.J. Chen, Effect of rubber substrates on the flexibility and tribological properties of diamond-like carbon coatings, Surf. Coat. Technol. 422 (2021), 127526.
[4] Y.T. Pei, D. Galvan, J.T.M. De, Hosson. Reactive magnetron sputtering deposition and columnar growth of nc-TiC/a-C: H nanocomposite coatings, J. Vac. Sci. Technol. A 24 (2006) 1448.
[5] Y.T. Pei, P. Huizenga, D. Galvan, J.T.M. De Hosson, Breakdown of the Coulomb friction law in TiC/a-C: H nanocomposite coatings, J. Appl. Phys. 100 (2006).
[6] J.C. Sanchez-Lopez, S. Dominguez-Meister, T.C. Rojas, et al., Tribological properties of TiC/a-C: H nanocomposite coatings prepared via HiPIMS, Appl. Surf. Sci. 440 (2018) 458–466.
[7] A.A. Voevodin, J.S. Zabinski, Load-adaptive crystalline–amorphous nanocomposites, J. Mater. Sci. 33 (2) (1998) 319–327.
[8] Y.T. Pei, X.L. Bui, X.B. Zhou, et al., Tribological behavior of W-DLC coated rubber seals, Surf. Coat. Technol. 202 (9) (2008) 1869–1875.
[9] W. Precht, A. Czyzniewski, Deposition and some properties of carbide/amorphous carbon nanocomposites for tribological application, Surf. Coat. Technol. 174–175 (2003) 979–983.
[10] A.A. Voevodin, et al., Design of a Ti/TiC/DLC functionally gradient coating based on studies of structural transitions in Ti–C thin films, Thin Solid Films 298 (1-2) (1997) 107–115.
[11] Y.J. Jo, et al. Synthesis and electrochemical properties of Ti-doped DLC films by a hybrid PVD/PECVD process. Applied Surface Science 433.mar.1(2018):1184-1191.
[12] K. Wang, H. Zhou, K. Zhang, et al. Effects of Ti interlayer on adhesion property of DLC films: A first principle study. Diamond and Related Materials 111(2021): 108188.
[13] H. Maruno, A. Nishimoto, Adhesion and durability of multi-interlayered diamond-like carbon films deposited on aluminum alloy, Surf. Coat. Technol. 354 (2018) 134–144.
[14] J.Q. Liu, L.J. Li, B. Wei, F. Wen, H.T. Cao, Y.T. Pei, Effect of sputtering pressure on the surface topography, structure, wettability and tribological performance of DLC films coated on rubber by magnetron sputtering, Surf. Coat. Technol. 365 (2019) 33–40.
[15] S.D. Zhang, M.F. Yan, Y. Yang, Y.X. Zhang, F.Y. Yan, H.T. Li, Excellent mechanical, tribological and anti-corrosive performance of novel Ti-DLC nanocomposite thin films prepared via magnetron sputtering method, Carbon 151 (2019) 136–147.
[16] Y.M. Wu, J.Q. Liu, H.T. Cao, Z.Y. Wu, Q. Wang, Y.P. Ma, H. Jiang, F. Wen, Y.T. Pei, On the adhesion and wear resistance of DLC films deposited on nitrile butadiene rubber: A Ti-C interlayer, Diamond & Related Materials 101 (2020), 107563.
[17] A.A. Voevodin, S.D. Walck, J.S. Zabinski, Architecture of multilayer nanocomposite coatings with super-hard diamond-like carbon layers for wear protection at high contact loads, Wear. 203 (1997) 516–527.
[18] B.J. Birscoe, K.S. Sebastian, M.J. Adams, The effect of indenter geometry on the elastic response to indentation, J. Phys. D: Appl. Phys. 27 (1994) 1156–1162.
[19] W.C. Oliver, G.M. Pharr, Measurement of Hardness and Elastic Modulus by Instrumented Indentation: Advances in Understanding and Refinements to Methodology, J. Mater. Res. 19 (2004) 3–20.
[20] W.C. Oliver, G.M. Pharr, An improved technique for determining hardness and elastic modulus using load and displacement sensing indentation experiments, J. Mater. Res. 7 (06) (1992) 1564–1583.
[21] A. Modabberasl, P. Kameli, M. Ranjbar, H. Salamati, R. Ashiri, Fabrication of DLC thin films with improved diamond-like carbon character by the application of external magnetic field, Carbon 94 (2015) 485–493.
[22] J. Robertson, Deposition mechanisms for promoting sp3 bonding in diamond-like carbon, Diam. Relat. Mater. 5–7 (1993) 984–989.
[23] J. Robertson, Diamond-like amorphous carbon, Mater. Sci. Eng. R Reports. 37 (2002) 129–281.
[24] A. Leyland, A. Matthews, On the significance of the H/E ratio in wear control: a nanocomposite coating approach to optimised tribological behaviour, Wear 246 (2000) 1–11.
[25] S. Kumar, N. Dwivedi, C. Rauthan, Investigation of radio frequency plasma for the growth of diamond like carbon films, Phys. Plasmas. 19 (3) (2012), 033515.
[26] N. Dwivedi, S. Kumar, H.K. Malik, Superhard behaviour, low residual stress, and unique structure in diamond-like carbon films by simple bilayer approach, J. Appl. Phys. 112 (2) (2012), 023518.
[27] X.L. Hu, A. Martini, Atomistic simulation of the effect of roughness on nanoscale wear, Comp. Mater. Sci. 102 (2015) 208–212.
[28] J. Musil, Hard and superhard nanocomposite coatings, Surf. Coat. Technol. 125 (2000) 322–330.
[29] C. Casiraghi, A.C. Ferrari, J. Robertson, Raman spectroscopy of hydrogenated amorphous carbon, Phys. Rev. B. 72 (8) (2005), 085401.
[30] N. Dwivedi, S. Kumar, H.K. Malik, Nanoindentation measurements on modified diamond-like carbon thin films, Appl. Surf. Sci. 257 (23) (2011) 9953–9959.
[31] S.T. Oktay, N.P. Suh, Wear Debris Formation and Agglomeration, J. Tribol. 114 (1992) 379–393.
[32] A.C. Ferrari, J. Robertson, Interpretation of Raman spectra of disordered and amorphous carbon, Phys. Rev. B 61 (20) (2000) 14095.
[33] J. Xu, J.W. Liu, X. Zhang, P. Ling, K. Xu, L. He, S. Su, Y. Wang, S. Hu, J. Xiang, Chemical imaging of coal in micro-scale with Raman mapping technology, Fuel 264 (2020), 116826.